

Two Class Motor Imagery Classification via Wave Atom Sub-Bands

Nebi Gedik

Abstract—The goal of motor image brain computer interface research is to create a link between the central nervous system and a computer or device. The most important signal for brain-computer interface is the electroencephalogram. The aim of this research is to explore a set of effective features from EEG signals, separated into frequency bands, using wave atom sub-bands to discriminate right and left-hand motor imagery signals. Over the transform coefficients, feature vectors are constructed for each frequency range and each transform sub-band, and their classification performances are tested. The method is validated using EEG signals from the BCI competition III dataset IIIa and classifiers such as support vector machine and k-nearest neighbors.

Keywords—Motor imagery, EEG, wave atom transform sub-bands, SVM, k-NN.

I. INTRODUCTION

THE goal of motor image (MI) brain computer interface (BCI) research is to create a link between the central nervous system and a computer or device. The most important signal for brain-computer connections is the electroencephalogram (EEG). While BCI studies benefit people with health problems by providing support and treatment, they also benefit healthy people by providing robotic control and enjoyment [1]-[4].

To efficiently transform recorded EEG signals into device commands, MI-based BCI devices require a good feature extraction and classification method. Athif et al. [5] offer WaveCSP, a machine learning strategy that employs wavelet transform and common spatial pattern (CSP) filtering algorithms to extract 24 characteristics from EEG signals. WaveCSP extracts information from the mu-beta rhythm of EEG using wavelet transform and CSP methods. The goal is to enhance the number of features to capture intra-band temporal and frequency domain class distinction. The performance of left versus right hand clenching MI classification is evaluated using the recommended EEG approach. To improve the performance of the SRC method for MI EEG classification, Miao et al. [6] focus on optimizing CSP features in subject-adapted space-frequency-time patterns and provide a detailed design for a more incoherent dictionary proposing spatial-frequency-temporal optimized feature sparse representation-based classification (SFTOFSRC) method. Al-Faiz et al. [7] uses four main processing steps to decode two-class motor imagery: 1- The raw EEG signal is decomposed into single trials, and spatial filters are estimated for each trial using CSP method; 2- features

are extracted using the log transformation (normal distribution) of the spatially filtered EEG signal; 3- an optimal channel selection algorithm is proposed to reduce the number of EEG channels; 4- finally, to distinguish between two classes of left and right hand MI, a support vector machine (SVM) is used. Polynomial function Kernel and radial-based function RBF Kernel are two SVM variants that have been proposed. Wang et al. [8] proposed a validation section for a deep convolutional neural network (CNN) that can categorize MI EEG signals. Based on EEG power spectrum data, a 6-layer CNN model is built to characterize MI tasks (left-right hand movement). The findings are compared to three other classic classification systems' results (LDA, SVM and MLP). Li et al. [9] proposes an adaptive feature extraction method based on wavelet packet decomposition (WPD) and SE-isomap. Through average power spectrum analysis, the MI-EEG is preprocessed to select a more effective time interval. The subject-based optimum wavelet packets (OWPs) with top mean variance difference are then obtained autonomously after WPD is applied to the specified segment of MI-EEG. The OWP coefficients are also utilized to statistically calculate time-frequency features and obtain nonlinear manifold structure features, as well as explicit nonlinear mapping, via SE-isomap. A k-nearest neighbor (k-NN) classifier is used to evaluate the hybrid features. Cheng et al. [10] offer a feature extraction method that combines principal component analysis (PCA) and deep belief networks (DBN). Initially, the second-order moment is applied to the time-domain of MI-EEG in order to determine the effective time interval. Then, PCA is used to examine the chosen time-domain period and determine the principal component feature points. The feature points are then transferred into DBN to complete the feature extraction process. Finally, classification is carried out using the softmax classifier. The BCI Competition II Data set III and BCI Competition IV Data set 2b are used to validate the algorithms.

The current study provides a multi-scale analysis-based feature extraction approach for identifying motor imagery EEG signals. Raw EEG signals are divided into four frequency bands, and each frequency range is subjected to a wave-atom transform to separate EEG data into sub-bands. To generate feature data, feature vectors are created using transform coefficients. SVM and k-NN classifiers, as well as BCI Competition III Data set IIIa, are used to validate the algorithm's classification of left- and right-hand motor imagery EEG data.

Nebi Gedik is with the University of Health Sciences, Institute of Hamidiye Health Sciences, Turkey (e-mail: nebi.gedik@sbu.edu.tr).

II. MATERIAL AND METHOD

A. Dataset

BCI competition III [11] used the motor imagery EEG data in this paper. BCI technology competitions are established to ensure that diverse data analysis approaches are assessed and to support the development of BCI technology. Various data sets are made available to everyone on the internet throughout each tournament, and each data set is a record of brain signals prepared in experienced and top BCI facilities. The labeled data partition, the "training set," and the unlabeled data partition, the "test set," make up these records. It comprises data on the right hand, left hand, foot, and tongue from three different participants. In each class, there are also 60 channels and 60 trials [12]. EEG signals are recorded using a 64-channel EEG amplifier, with the left mastoid serving as the reference and the right mastoid serving as the ground. Fig. 1 depicts the channel placements.

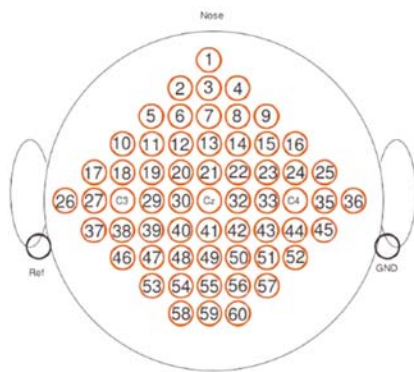


Fig. 1 Channel positions for the data set IIIa of the BCI competition III [12]

The experiment is carried out while creating the dataset and comprises of numerous runs (at least 6) with 40 trials each. The first two seconds of the trial are silent; then, at $t=2s$, an acoustic stimulus indicates the start of the trial and a cross "+" is displayed; then, from $t=3s$, an arrow to the left, right, up, or down is displayed for 1s; and, at the same time, the subject is asked to imagine a left hand, right hand, tongue, or foot movement until the cross disappears at $t=7s$ [12]. Fig. 2 depicts the procedure.

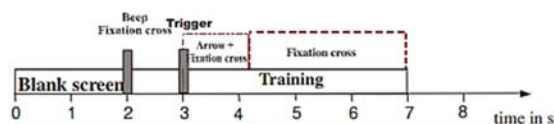


Fig. 2 The paradigm's timeline [12]

B. Wave Atom Transform

Demanet and Ying presented the wave atom transform in [13], which belongs to the family of directed multi-scale transforms. The transform is a parabolic scaling relation variation of 2-D wavelet packets, in which the wavelength is proportional to the square of the diameter. Wave atoms generate an expansion of oscillatory functions or oriented textures that are much sparser than any other multi-resolution

representations, in addition to having superior frequency localization, which is a concern for filter banks.

Among the several available transforms, the wave atom transform is defined by two parameters, α and β . Most known wave packet topologies may be classified using these parameters. The links between various transforms have been elucidated using this explanation. These parameters indicate whether the decomposition is multi-scale ($\alpha = 1$) or not ($\alpha = 0$), as well as if it is poorly directional ($\beta = 1$) or totally directional ($\beta = 0$). Fig. 3 depicts the classification of multi-resolution transforms according to α and β [13].

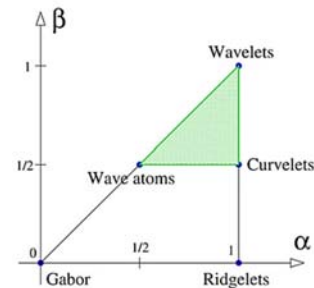


Fig. 3 According to (α, β) , the structures of several wave packets are depicted III [13]

The tensor products of 1D wave packets make up wave atoms. Ortho-normal basis functions with the subscript $\mu = (j, m, n)$ are used to produce two-dimensional wave atoms $\varphi_{\mu}(x_1, x_2)$. The wave atom tight frame is created by combining the basis function and its Hilbert-transformed version [13].

$$\varphi_{\mu}^1 = \frac{\varphi_{\mu}^+ + \varphi_{\mu}^-}{2}, \varphi_{\mu}^2 = \frac{\varphi_{\mu}^+ - \varphi_{\mu}^-}{2} \quad (1)$$

C. Proposed Method

The BCI competition III dataset IIIa provided the motor imagery EEG dataset used in this investigation. From three people, the dataset has four types of motor imagery EEG data. Those are right hand (rh), left hand (lh), foot, and tongue. This research, on the other hand, focused on the classification of rh and lh imagery signals classification among them. So, first, the EEG data, which contains the rh and lh motor imagery information, is extracted from the data set, and then a new data set is constructed utilizing them. This new data set containing 60 channel signal information, as a further operation for dataset preparing, is rebuilt using three channels (C3, C4, and Cz), which is also preferred in the literature [14], [15]. The dataset consists of the signal from the C3, C4, and Cz electrodes is separated into four frequency bands, and the wave atom transform is applied to the data in each frequency range to decompose the data into five sub-bands. The feature data sets, totaling 9 feature sets, are then constructed by computing standard deviation (sd), entropy (en), and log-variance (lv) for each sub-band in each frequency range separately from the transformation coefficients. Every feature set is classified using SVM and k-NN (k-value starts with 3 and accepts 30 different values) algorithms. Fig. 4 shows the flow chart for the procedure.

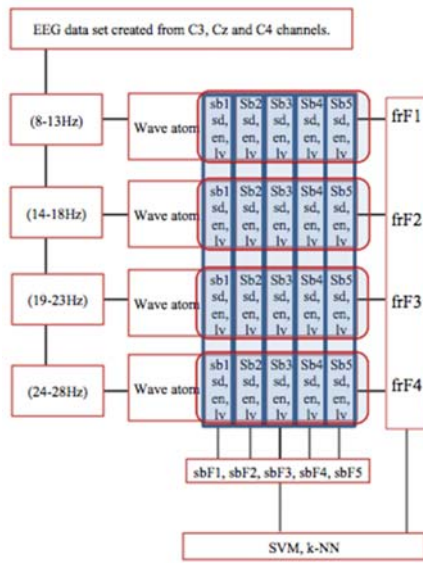


Fig. 4 The flow chart of the method expressed in this paper. Where sbFx express xth sub-bands feature i.e. $sbF1 = sb1^{8-13Hz} + sb1^{14-18Hz} + sb1^{19-23Hz} + sb1^{24-28Hz}$, frFx express frequency range feature i.e. $frF1 = sb1 + sb2 + sb3 + sb4 + sb5$

III. FINDINGS

After transferring the selected channel signals to the four frequency bands and performing the wave atom transform, the sd, en, and lv values for each sub-band are calculated separately across the transform coefficients. Nine feature sets are reproduced and used to feed classifiers one by one. The success rates of the sub-bands wise classification are shown in Table I. Table II shows the classification findings by frequency range.

TABLE I
 THE CLASSIFICATION RESULTS FOR THE FEATURES FROM EACH SUB-BANDS

Feature set	Subject	SVM	k-NN	k
sbF1	Subject 1	55,55	58,89	13
	Subject 2	58,33	56,67	5
	Subject 3	50	56,67	27
sbF2	Subject 1	51,11	57,78	13
	Subject 2	63,33	60	39
	Subject 3	55	58,33	3
sbF3	Subject 1	64,44	63,33	39
	Subject 2	56,67	55	33
	Subject 3	58,33	58,33	25
sbF4	Subject 1	70	56,67	17
	Subject 2	58,33	63,33	37
	Subject 3	68,33	63,33	13
sbF5	Subject 1	56,67	60	15
	Subject 2	63,33	63,33	3
	Subject 3	51,67	60	23

TABLE II
 THE CLASSIFICATION RESULTS FOR THE FEATURES FROM EACH FREQUENCY RANGES

Feature set	Subject	SVM	k-NN	k
frF1	Subject 1	62,22	64,44	33
	Subject 2	50	58,33	17
	Subject 3	63,33	56,67	35
frF2	Subject 1	65,56	65,56	23
	Subject 2	63,33	66,67	41
	Subject 3	60	58,33	33
frF3	Subject 1	62,22	58,89	7
	Subject 2	60	58,33	25
	Subject 3	60	58,33	7
frF5	Subject 1	65,56	56,67	19
	Subject 2	66,67	63,33	41
	Subject 3	53,33	56,67	39

In terms of overall classification performance, the SVM classifier utilizing feature data from subject one and wave atom sub-bands 4 (sbF4) has the best classification performance. However, in both classifiers, the averages of classification results by sub-bands (ie with sbFxs) remain lower than the average of classification results by frequency range (ie with frFxs). When it comes to the subjects, the sub-band feature set sbF4 again provides the best average of classification success for the three subjects.

IV. CONCLUSION

The success of the sub-bands of the wave atom transform in the classification of motor imagery EEG data comprising right- and left-hand motor imagery information is studied in this work. The signals are decomposed into five sub-bands using the wave atom transform after the three-channel EEG data is split into four frequency bands. The nine feature data sets are created using the coefficients of each sub-band considering frequency ranges. As a consequence of the classification processes, the best classification performance is obtained from SVM classifier with feature data from subject one and wave atom sub-bands 4.

REFERENCES

- [1] J. R. Millan, et al. "Noninvasive brain-actuated control of a mobile robot by human EEG." *IEEE Transactions on biomedical Engineering*, vol. 51, no.6, pp.1026-1033, 2004.
- [2] J. R. Wolpaw, et al. "Brain-computer interfaces for communication and control." *Clinical neurophysiology*, vol.113, no.6, pp. 767-791, 2002.
- [3] A. Finke, A. Lenhardt, H. Ritter. "The MindGame: a P300-based brain-computer interface game." *Neural Networks*, vol.22, no.9, pp. 1329-1333, 2009.
- [4] J. J. Daly, J. E. Huggins, "Brain-computer interface: current and emerging rehabilitation applications." *Arch Phys Med Rehabil*, vol. 96, no. 3, pp. 1-7, 2015.
- [5] M. Athif, H. Ren, "WaveCSP: a robust motor imagery classifier for consumer EEG devices." *Australas Phys Eng Sci Med.*, vol. 42, no. 1, pp. 159-168, 2019.

- [6] M. Miao, A. Wang, F. Liu, "A spatial-frequency-temporal optimized feature sparse representationbased classification method for motor imagery EEG pattern recognition." *Med Biol Eng Comput*, vol. 55, no. 9, pp. 1589-603, 2017.
- [7] M. Z. Al-Faiz, A. A. Al-hamadani. "Implementation of EEG signal processing and decoding for twoclass motor imagery data." *Biomed Eng Appl Basis Commun*, vol. 31, no. 4, p.1950028, 2019.
- [8] J. Wang, G. Yu, L. Zhong, W. Chen, Y. Sun, "Classification of EEG signal using convolutional neural networks", in *14th IEEE Conference on Industrial Electronics and Applications*, pp. 1694-1698, 2019.
- [9] M. Li, W. Zhu, H. Liu, and J. Yang, "Adaptive feature extraction of motor imagery EEG with optimal wavelet packets and SE-isomap," *Applied Sciences*, vol. 7, no. 390, pp. 1-18, 2017.
- [10] L. Cheng, D. Li, G. Yu, Z. Zhang, X. Li, and S. Yu, "A motor imagery EEG feature extraction method based on energy principal component analysis and deep belief networks," *IEEE Access*, vol. 8, pp. 21453–21472, 2020.
- [11] BCI competition III, <http://www.bbc.de/competition/iii/> (last accessed 20.11.2021).
- [12] BCI competition III dataset IIIa, http://www.bbc.de/competition/iii/desc_IIIa.pdf (last accessed 20.11.2021)
- [13] L. Demanet, and L. Ying, "Wave atoms and sparsity of oscillatory patterns," *Applied and Computational Harmonic Analysis*, vol. 23, no. 3, pp. 368-387, 2007.
- [14] J. Jin, Y. Miao, I. Daly, C.D. Hu, A. Cichocki, "Correlation-based channel selection and regularized feature optimization for MI-based BCI," *Neural Networks*, vol.118, pp.262-270, 2019.
- [15] G. Pfurtscheller and F. L. Da Silva, "Event-related EEG/MEG synchronization and desynchronization: Basic principles", *Clin. Neurophysiol.*, vol. 110, no. 11, pp. 1842-1857, 1999.

Nebi Gedik received his B.S. degree in Electrical and Electronics Engineering from Firat University in 2001, his PhD degrees in Electrical and Electronics Engineering from Karadeniz Technical University in 2013, and his MSc degree in 2005 from Atatürk University. He is now an Associate Professor at University of Health Science. His research interest includes medical image and signal processing, pattern recognition and machine learning.